A NUMERICAL STUDY OF THE INFLUENCE OF THE VOID DRIFT MODEL ON THE PREDICTIONS OF THE ASSERT SUBCHANNEL CODE

P. TYE[1], A. TEYSSEDOU[1], N. TROCHE[1], & J. KITELEY[2]

(1) Institut de génie nucléaire,
Département de génie mécanique, École Polytechnique,
C.P. 6079, succ. Centre–ville, Montréal, Québec, CANADA H3C 3A7

(2) CANDU Technology, FUEL AND FUEL CYCLE DIVISION,
Fuel Channel Thermalhydraulics Branch,
Atomic Energy of Canada Limited
Chalk River Laboratories, Chalk River Ontario, CANADA, K0J–1J0

ABSTRACT

One of the factors which is important in order to ensure the continued safe operation of nuclear reactors is the ability to accurately predict the "Critical Heat Flux" (CHF) throughout the rod bundles in the fuel channel. One method currently used by the Canadian nuclear industry to predict the CHF in the fuel bundles of CANDU reactors is to use the ASSERT subchannel code to predict the local thermal–hydraulic conditions prevailing at each axial location in each subchannel in conjunction with appropriate correlations or the CHF look–up table. The sucessfull application of the above methods depends greatly on the ability of ASSERT to accurately predict the local flow conditions throughout the fuel channel.

In this paper, full range qualitative verification tests, using the ASSERT subchannel code are presented which show the influence of the void drift model on the predictions of the local subchannel quality. For typical cases using a 7 rod subset of a full 37 element rod bundle taken from the ASSERT validation database, it will be shown that the void drift term can significantly influence the calculated distribution of the quality in the rod bundle. In order to isolate, as much as possible, the influence of the void drift term this first numerical study is carried out with the rod bundle oriented both vertically and horizontally. Subsequently, additional numerical experiments will be presented which show the influence that the void drift model has on the predicted CHF locations.

1. Introduction

In CANDU reactors the coolant flowing through the fuel bundles may boil during normal operating conditions thus creating a horizontal two-phase flow. Of particular importance is the ability to accurately predict the CHF location in the fuel bundle. CHF defines the condition under which the heat transfer mechanism from the fuel element to the coolant deteriorates. This condition may result in a very high and rapid temperature rise, which may endanger the fuel integrity. One method used to predict the CHF in the fuel bundles of CANDU reactors is to use the ASSERT subchannel code to predict the local thermal–hydraulic conditions prevailing at each axial location in each subchannel in conjunction with appropriate correlations or the CHF look–up table [1]. The sucessfull application of the above methods depends greatly on the ability of ASSERT to accurately

predict the local flow conditions throughout the fuel channel.

ASSERT solves the one dimensional conservation equations of mass, momentum and energy for each subchannel while taking into account the possible inter–subchannel interactions as source terms to these 1-D equations. These interactions are [2,3]:

i) Diversion Crossflow: which is the directed flow caused by pressure differences between the subchannels.

ii) Turbulent Void Diffusion: This mechanism is analogous to the mixing due to turbulence in single phase flow. However, in two–phase flow this mixing mechanism may lead to a net mass exchange due to the differences in the average mixture densities in adjacent subchannels.

iii) Void Drift: This mechanism accounts for the tendency of the vapor phase to shift to higher velocity subchannels.

iv) Buoyancy Drift: In horizontal channels, the void is pushed upwardly normal to the major flow direction due to the difference in the densities of the two phases.

One of the motivations for this study comes from the fact that while it has been found that the ASSERT predictions of the critical power at high flows are quite good [3], the same cannot be said for lower flows. Furthermore, while the predicted axial location of first dryout have been found to be in good agreement with experimental results, the agreement was not as good concerning the radial locations of the first dryout. It has been suggested [4] that the possible culprit for this lack of agreement is the void drift model. Thus, in this paper, full range qualitative verification tests, using the ASSERT subchannel code are presented which show the influence of the void drift model on the predictions of the local subchannel quality. This study is carried out using a 7 rod subset of a full 37 rod bundle taken from the ASSERT validation database, it will be shown that the void drift term can significantly influence the calculated distribution of the quality in the rod bundle. In order to isolate the influence of the void drift term this numerical study is carried out with the bundle oriented both vertically, i.e. no buoyancy drift, and horizontally which show the influence that combination of both the void drift and the buoyancy drift have on the predicted quality distribution in the rod bundle. Additional numerical experiments are presented which show the influence that the void drift model has on the predicted CHF locations. While this study concentrates on void drift it is equaly important to correctly model turbulent void diffusion and buoyancy drift.

2. ASSERT subchannel code

ASSERT uses an advanced drift flux model which permits cases involving both thermal and mechanical non–equilibrium to be considered. ASSERT is, at the level of the individual subchannels a one dimensional two–phase flow code, however, at the level of the fuel bundle it has a three dimensional nature. This three–dimensional representation of the fuel bundles is arrived at by including the effects of the crossflow as source terms in the 1–D form of the conservation equations of mass, axial momentum and energy, and by the addition of a transverse momentum equation. The equations of conservation of mass, axial and transverse momentum and mixture energy as applied in ASSERTgiven below.

i) Conservation of Mass for subchannel *i*:

$$A_i \frac{\partial}{\partial t}\rho_{mi} + \frac{\partial}{\partial x}F_i + \sum_{j=1}^{n} W_{ij} = 0 \ . \tag{1}$$

ii) Conservation of Axial Momentum for subchannel *i*:

$$\frac{\partial}{\partial t}F_i + \frac{\partial}{\partial x}\frac{F_i^2}{A_i\rho_{mi}} + \frac{\partial}{\partial x}A_i\frac{\alpha_i\,(1-\alpha_i)\rho_\ell\rho_g}{\rho_{mi}}u_{ri}^2 + \sum_{j=1}^{n} W_{ij}u_m^*$$

$$+\sum_{j=1}^{n} s\frac{\alpha^*\,(1-\alpha^*)\,\rho_\ell^*\rho_g^*}{\rho_m^*}v_{rij}u_r^* = -A_i\frac{\partial}{\partial x}p_i - \mathcal{F}_{ai} - A\rho_{mi}g\cos\theta \quad , \tag{2}$$

where F_i is the mixture mass flow rate, W_{ij} is the crossflow, ρ_{mi} is the mixture density, and $\mathcal{F}_{ai}$ represents the axial frictional loss terms.

iii) Conservation of Transverse Momentum:

$$\frac{\partial}{\partial t}W_{ij} + \frac{\partial}{\partial x}W_{ij}\overline{u_m} + \frac{\partial}{\partial x}s\left[\frac{\alpha^*(1-\alpha^*)\rho_\ell^*\rho_g^*}{\rho_m^*}\right]\overline{u_r}v_{rij} =$$

$$-\frac{\bar{s}}{\ell}(p_j - p_i) - \frac{\bar{s}}{\ell}\mathcal{F}_{tij} - \bar{s}\,\overline{\rho_m}g\sin\theta\cos\phi \quad , \tag{3}$$

where θ represents the bundle orientation, ϕ is the angle of the inter–subchannel gap, $\mathcal{F}_{tij}$ represents the transverse frictional loss terms, and the superscript * indicates donor assignment of the quantity.

ii) Conservation of Mixture Energy for subchannel *i*: (Transportive Form)

$$A_i\rho_{mi}\frac{\partial}{\partial t}h_{mi} + F_{mi}\frac{\partial}{\partial x}h_{mi} + \frac{\partial}{\partial x}A_i\frac{\alpha_i\,(1-\alpha_i)\rho_\ell\rho_g}{\rho_{mi}}(h_{vi} - h_{li})u_{ri} - h_{mi}\sum_{j=1}^{n} W_{ij}$$

$$+\sum_{j=1}^{n} W_{ij}h_m^* = -\sum_{j=1}^{n} W_l'(h_{lj} - h_{li}) - \sum_{j=1}^{n} W_g'(h_{gj} - h_{gi}) + Q_i'' \quad , \tag{4}$$

Additional equations also exit for the transport of phasic energy. Details on the solution scheme as applied in ASSERT are presented in Webb and Rowe [5].

3. Constitutive relations

In developing the equations used in ASSERT a large number of simplifying assumptions were made. Each of these assumptions results in a loss of some fundamental information which must then be replaced by closure relations. In particular closure relationships for the inter–subchannel interchange mechanisms are required. These include relations for: 1) the transverse relative velocity, 2) the buoyancy drift, 3) the turbulent void diffusion, and 4) the void drift. Items 2, 3, and 4 are represented as contributions to item 1. The general form of the relative velocity is given by :

$$\vec{V}_r = \frac{(C_o - 1)\vec{j}}{(1-\alpha)} + \frac{\vec{V}_{gj}}{(1-\alpha)} - \frac{\epsilon}{\alpha(1-\alpha)}\vec{\nabla}(\alpha - \alpha_{eq}) \quad , \tag{5}$$

where the first term represents the effect of cross sectional averaging, the second term is the buoyancy drift, and the third term represents a combination of both turbulent void diffusion and void drift.

3.1 Axial relative velocity

Since in the axial direction the void diffusion is negligible, the axial relative velocity is modeled using only the first two terms of equation (5) and is given by:

$$u_r = \frac{(C_o - 1)j}{(1-\alpha)} + \frac{u_{gj}}{(1-\alpha)} \quad . \tag{6}$$

3.2 Transverse relative velocity

The phase distribution coefficient, C_o, in the transverse direction is assumed to be equal to 1, which eliminates the first term of Equation (5), thus the transverse component of the relative velocity, $\vec{V}_r$, is given by:

$$v_r = \frac{v_{gj}}{(1-\alpha)} - \frac{\epsilon}{\alpha(1-\alpha)} \frac{\partial}{\partial y}(\alpha - \alpha_{eq}) \quad . \tag{7}$$

The drift velocity, v_{gj}, used to represent the buoyancy drift mechanism is expressed using a variation of Wallis's [6] model for the terminal rise velocity of a bubble and is given by:

$$v_{gj} = 1.5F(\bar{\alpha})^{0.1} \left(\frac{\rho_\ell - \rho_g}{\rho_\ell^2} \sigma g \right)^{0.25} \cos\phi \quad , \tag{8}$$

where F is the Ohkawa–Lahey [6] correction factor used to drive $v_{gj} \rightarrow 0$ as $\alpha \rightarrow 1$.

The turbulent void diffusion coefficient, ϵ, in Equation (7) is specified using a correlation with the inverse turbulent Peclet number, and is given by:

$$\frac{\epsilon}{\overline{u_m}\,\overline{D_h}} = aRe^b \quad , \tag{9}$$

where $\overline{u_m}$ is the average velocity and $\overline{D_h}$ the average hydraulic diameter in the two subchannels under consideration, the recommended values of a and b are 0.05 and 0 respectively. Investigations of the Reynolds number dependency of the void diffusion turbulent mixing which will allow individual subchannel mixing to be modeled are currently underway.

In equation (7) the void diffusion and void drift terms for two subchannels i and j are calculated using the model presented in [2], where the equilibrium void fraction α_{EQ} for the i^{th} subchannel is calculated as:

$$\alpha_{iEQ} = \left[\frac{\bar{\alpha}}{\bar{G}_m} \right] G_{mi} \quad , \tag{10}$$

the average void fraction, $\bar{\alpha}$, and the average mass flux, $\bar{G}_m$, are calculated using subchannel flow area weighting which results in the following expressions:

$$\bar{\alpha} = \frac{(\alpha A)_i + (\alpha A)_j}{A_i + A_j} \quad \text{and} \quad \bar{G}_m = \frac{F_{mi} + F_{mj}}{A_i + A_j} \quad .$$

4. Results of Full Range Qualitative Verification Tests

The results of a number of full range qualitative verification tests carried out using the ASSERT subchannel code will now be presented. Figure 1 shows the geometry of the 7 rod bundle used for these tests.

4.1 Results of Quality Distribution Tests

The test matrix for the full range qualitative verification tests is shown in Table 1.

Outlet Pressure	5.5 & 10 MPa
Mass Flux	2, 4, & 6 $Mgm^{-2}s^{-1}$
Bundle Averaged Outlet Quality	18.0 %
Inlet Temperature	200 & 260 $^{\circ}C$

Table 1: Matrix for full range qualitative verification tests

In this paper only the results for the cases having mass fluxes of 2.0 and 6.0 $Mgm^{-2}s^{-1}$ are presented. Figures 2 and 3 show the results of the quality in subchannels 1 and 7 (see Figure 1) at a pressure of 5.5 MPa and a mass flux of 2.0 $Mgm^{-2}s^{-1}$ for vertical and horizontal flows respectively. Figures 4 and 5 show the same results for a mass flux of 6.0 $Mgm^{-2}s^{-1}$. It can be seen that for both mass fluxes, under vertical flow conditions, that the inclusion of the void drift mechanism in the lateral relative velocity calculation results in a much more uniform quality distribution than when this mechanism is neglected. Furthermore, it can also be seen that the mass flux has a relatively minor influence on the subchannel quality distribution in vertical flow. It can also be observed that when the void drift mechanism is neglected the difference in the subchannel qualities continues to increase along the entire length of the channel whereas for the case where the influence of this mechanism is included an almost constant quality difference is seen to be established between the two subchannels which is maintained up to the end of the channel.

Under horizontal flow conditions for both mass fluxes it can again be observed that an equilibrium difference in the subchannel qualities is also established towards the end of the channel when the void drift mechanism is taken into account. When the channel is oriented horizontally the influence of the gravity induced phase seperation, which occurs across the entire bundle, will tend to cause the mass flux in the lower regions of the bundle to be higher than in the upper regions. Under these conditions, the influence of the void drift mechanism is to provide an additional mechanism by which the distribution of the vapour phase, i.e. quality, can be made more uniform throughout the bundle. Examining Figure 3 (low mass flux) it can be seen that the quality is higher in both subchannels when the void drift mechanism is neglected. Here, the influence of the buoyancy drift is to drive the vapour into the top part of the bundle and the only mechanism which acts to redistribute the vapour more uniformly is turbulent void diffusion. Comparing Figures 3 and 5, it can be seen that at the higher mass flux the inclusion of the void drift mechanism has a much greater effect and that towards the end of the channel the vapour is distributed more

uniformly. This results is reasonable in view of the fact that, in ASSERT, the buoyancy drift is independent of the mass flux whereas the void drift is not. Therefore, at lower mass fluxes the tendency of the buoyancy drift to drive the vapour towards the top of the bundle will dominate. In fact it can be seen that at a mass flux of 2.0 $Mgm^{-2}s^{-1}$ (Fig. 3) the highest quality is found to occur in the physically higher subchannel (# 7) whereas for a mass flux of 6.0 $Mgm^{-2}s^{-1}$ (Fig. 5) the highest quality occurs in subchannel 1.

Figures 6 and 7 show the results of the quality in subchannels 1 and 7 (see Figure 1) at a pressure of 10.0 MPa and a mass flux of 2.0 $Mgm^{-2}s^{-1}$ for vertical and horizontal flows respectively. Figures 8 and 9 show the same results for a mass flux of 6.0 $Mgm^{-2}s^{-1}$. Again it is observed that for vertical flows the inclusion of the void drift mechanism results in a more uniform quality distribution in the subchannels and an equilibrium quality difference between the subchannels is established. For horizontal flows and for the mass flux of 6.0 $Mgm^{-2}s^{-1}$, when the void drift mechanism is taken into account, an equilibrium quality difference is reached towards the end of the channel, no such equilibrium is however reached at the lower mass flux. Comparing Figures 5 and 9 it can be seen that at higher pressures the equilibrium quality difference between the two subchannels is smaller. This is due to the combination of two factors, the first is that at higher pressures for the same quality the void fraction is lower. This means that the overall magnitude of the void transport mechanisms will also be lower. Furthermore, for any given void fraction buoyancy drift is less important at higher pressures due to a smaller density difference between the phases. Thus, the quality is distributed more evenly throughout the bundle.

4.1 Results of CHF Location Tests

The other set of qualitative verification tests which were carried out were done in order to determine the influence of the inclusion or exclusion of the void drift mechanism on the CHF location. Only two cases will be shown, the inlet test conditions are: Pressure 10 MPa, Mass Flux 4. $Mgm^{-2}s^{-1}$, $T_{in} = 260\ ^{\circ}C$, and a heat flux of 1.01 MW/m^2 with the channel oriented both vertically and horizontally. This heat flux corresponds to that required to reach dryout at the exit of the channel under horzontal flow conditions when the void drift mechanism is taken into account.

Figure 10 shows the case for vertical flow, when the void drift mechanism is neglected a much larger quality difference is seen between the two subchannels and no clear equilibrium quality distribution is seen. For this case CHF is predicted to occur at the end of the channel on rod #3 in subchannel 1. For the case when this mechanism is taken into account a clear equilibrium quality difference is established between the two subchannels and CHF is never reached. This is due to the more uniform quality distribution which results due to the influence of void drift.

Figure 11 shows the quality in subchannels 1 and 7 for the case of horizontal flow. When the void drift mechanisn is taken into account CHF is predicted to occur at the end of the channel on rod #3 in subchannel 7, while it is predicted to occur almost 50 cm upstream on rod # 2 in subchannel 1 when the void drift is neglected.

Figures 12 and 13 shows the lateral relative velocity and its components for cases of vertical and horizontal flow respectively. It is important to note that the relative velocity

and its components are defined as being positive from subchannel 1 to subchannel 7. Comparing Figures 12 and 13 it can be seen that the void drift component is larger, for this subchannel pair, under vertical flow conditions than under horizontal flow conditions. Examining Figure 13 it can be seen that the turbulent void diffusion is the dominant mechanism up to about 300 *cm* along the channel. At this point the buoyancy drift mechanism is seen to be the major contribution to the lateral relative velocity. Along the entire length of the channel it can be seen that the void drift component is never the dominant lateral transport mechanism.

5. Conclusions

A number of full range qualitative verification tests have been carried out in order to determine the influence of the void drift mechanism on the subchannel quality distribution under both vertical and horizontal conditions. The influence of this model on the CHF location for both vertical and horizontal flows have also been studied.

It has been shown that the void drift mechanism causes the quality distribution in the rod bundle to tend towards an equilibrium difference among the subchannels. Such equilibrium differences have been observed experimentally in both vertical [8, 9] and horizontal flow conditions [10].

It has been found [4], for horizontal flow conditions, that the when void drift is taken into account the predicted CHF locations are pushed towards the top of the rod bundle whereas experimentally it is seen to occur more towards the center. The present study does show that the inclusion of the void drift mechanism can modify the predicted CHF location.

However, in view of the fact that the void drift mechansim accounts for certain experimentally observed trends as well as its magnitude as compared to buoyancy and turbulent void diffusion the fact that the inclusion of this mechanism results in an incorrect prediction of the CHF location may be more of a case of an incremental affect rather than the root cause. If the quality is predicted to be higher in the upper subchannels than it is in reality and this results in the prediction of the wrong radial location of the CHF a more likely candidate for this is the buoyancy drift mechanism. In fact, a previous study [11] has shown that the buoyancy drift mechanism may be over estimated in ASSERT.

Acknowledgement

ASSERT was made available to École Polytechnique by agreement with the CANDU OWNERS GROUP, Fuel Channel Critical Power Working Party.

References

[1] D.C. Groeneveld, S.C. Cheng, and T. Doan, "The AECL-UO Critical Heat Flux Look–Up Table," Heat Transfer Eng., Vol. 7, No. 46, 1986.

[2] R.T. Lahey Jr. and J.F. Moody, " The Thermal–hydraulics of a Boiling Water Nuclear Reactor," (American Nuclear Society., N.Y., 1979) pp 122–138.

[3] M.B. Carver, J.C. Kiteley, R.Q.N. Zhou, S.V. Junop, and D.S. Rowe, "Validation of the ASSERT Subchannel Code: Prediction of Critical Heat Flux in Standard and Nonstandard CANDU Bundle Geometries," Nuclear Technology, Vol. 112, No. 3, Dec. 1995.

[4] J.C. Kiteley personal communication Jan. 1996.

[5] S.W. Webb and D.S. Rowe," Modeling techniques for dispersed multiphase flows," in: Encyclopedia of Fluid Mechanics, (Gulf Publishing Company, 1986) pp. 909–968.

[6] G.B. Wallis, "One Dimensional Two–Phase Flow," (McGraw Hill, N.Y., 1969) pp 248–255.

[7] K. Ohkawa, and R.T. Lahey Jr., " The analysis of CCFL using drift–flux models," Nucl, Eng. Des. 61 (1980) 245–255.

[8] R.T. Lahey Jr. and F.A. Schraub, " Mixing, Flow Regimes and Void Fraction for Two–Phase Flow in Rod Bundles," ASME Booklet, Two–Phase Flow and Heat Transfer in Rod Bundles, (1969).

[9] R.W. Sterner and R.T. Lahey Jr., "Air/Water Subchannel Measurements of the Equilibrium Quality and Mass Flux Distribution in a Rod Bundle," NUREG/CR–3373, (1983).

[10] A. Tapucu, M. Geçkinli, N. Troche, and R. Girard, "Experimental investigation of mass exchanges between two laterally interconnected two–phase flows," Nucl. Eng. Des. 105 (1988) 295–312.

[11] P.Tye, A. Teyssedou, and A. Tapucu, "An investigation of the constitutive relations for intersubchannel transfer mechansims in horizontal flows as applied in the ASSERT–4 subchannel code," Nucl. Eng. Des. 149 (1994) 207–220.

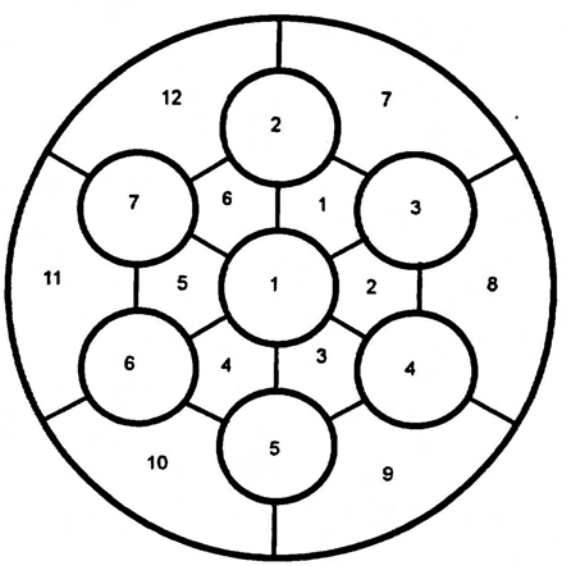

Figure 1. 7 Rod Bundle (Subset of 37 Element CANDU Bundle).

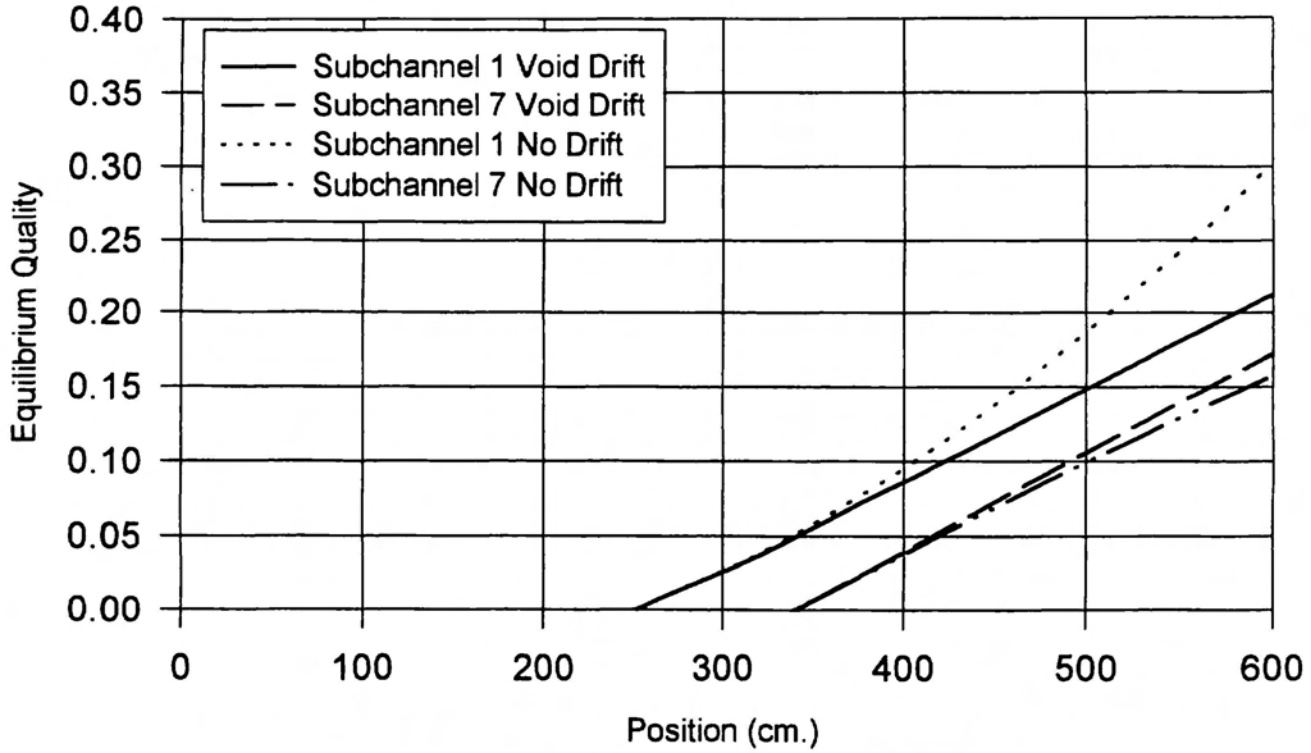

Figure 2. Influence of Void Drift on Subchannel Quality
P=5.5 MPa, G=2.0 Mg/m^2/s, T_{in}=200 °C
Vertical Flow.

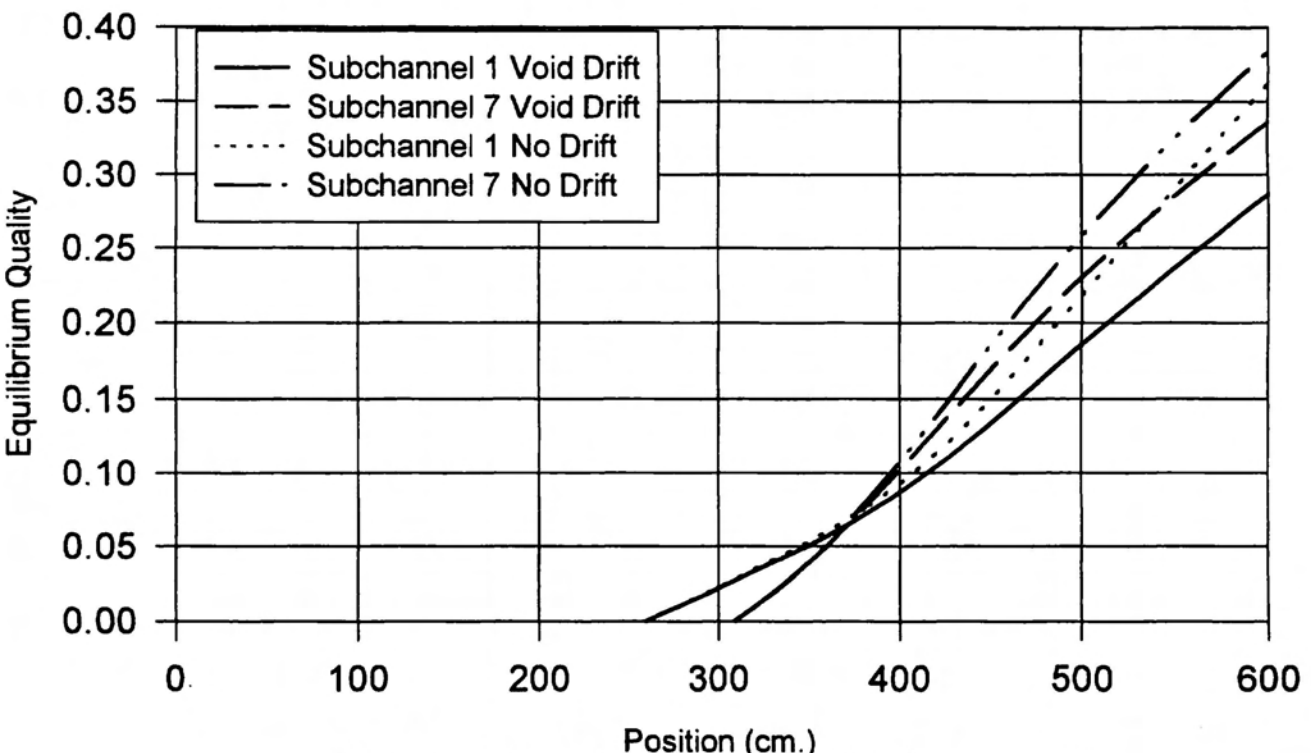

Figure 3. Influence of Void Drift on Subchannel Quality
P=5.5 MPa, G=2.0 Mg/m^{2}s, T_{in}=200 °C
Horizontal Flow.

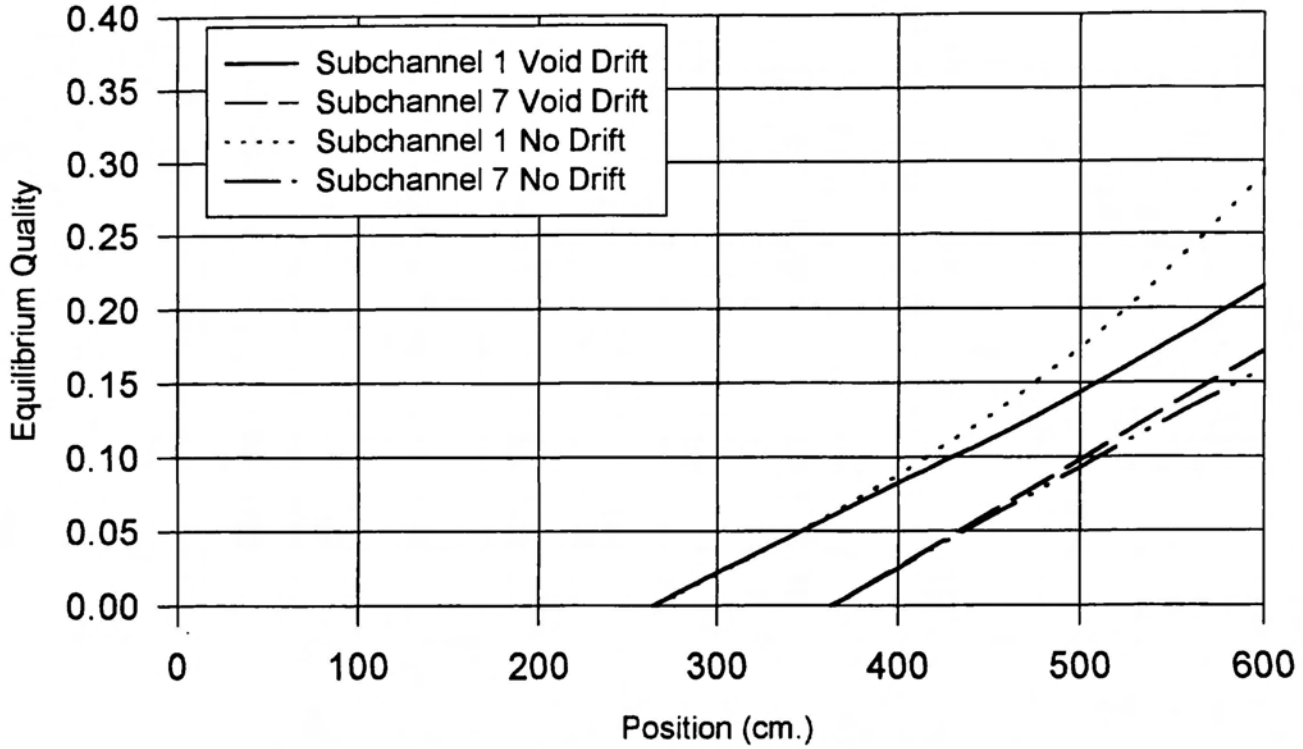

Figure 4. Influence of Void Drift on Subchannel Quality
P=5.5 MPa, G=6.0 $Mg/m^2/s$, T_{in}=200 °C
Vertical Flow

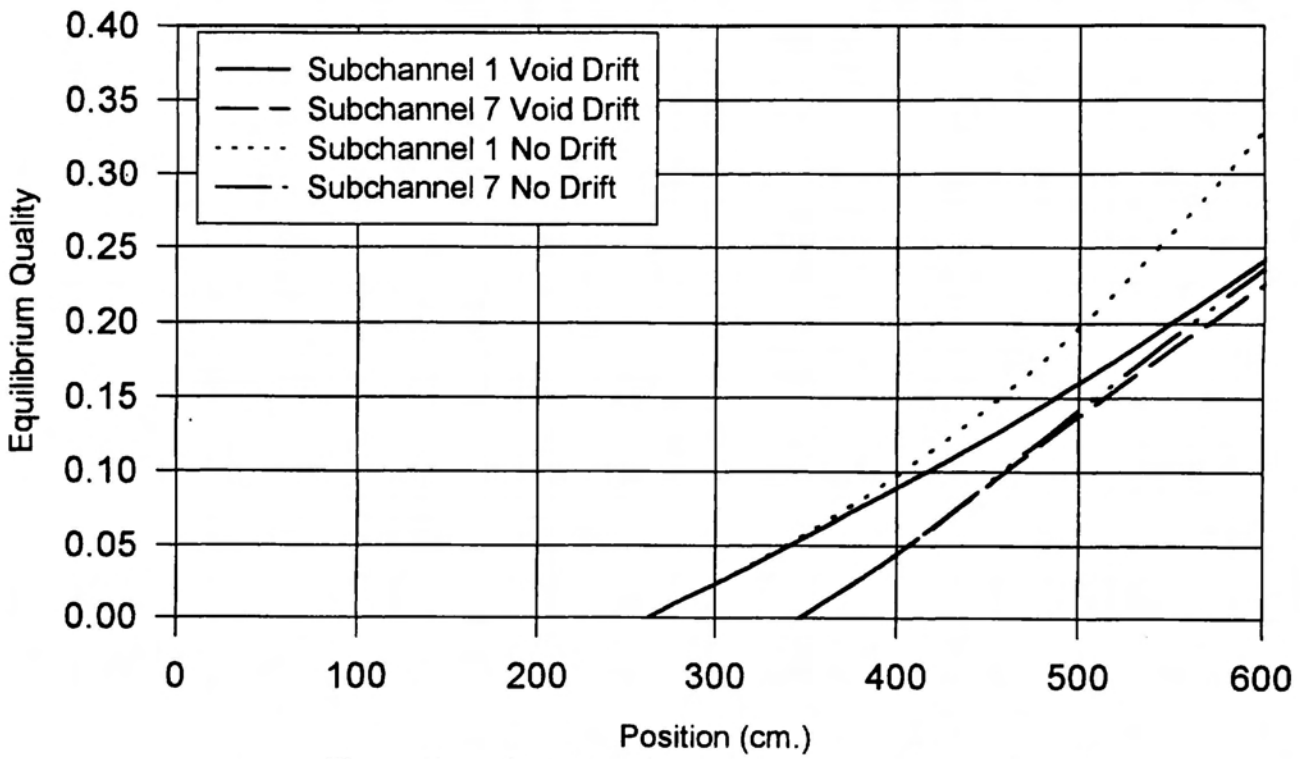

Figure 5. Influence of Void Drift on Subchannel Quality
P=5.5 MPa, G=6.0 Mg/m^2s, T_{in}=200 °C
Horizontal Flow

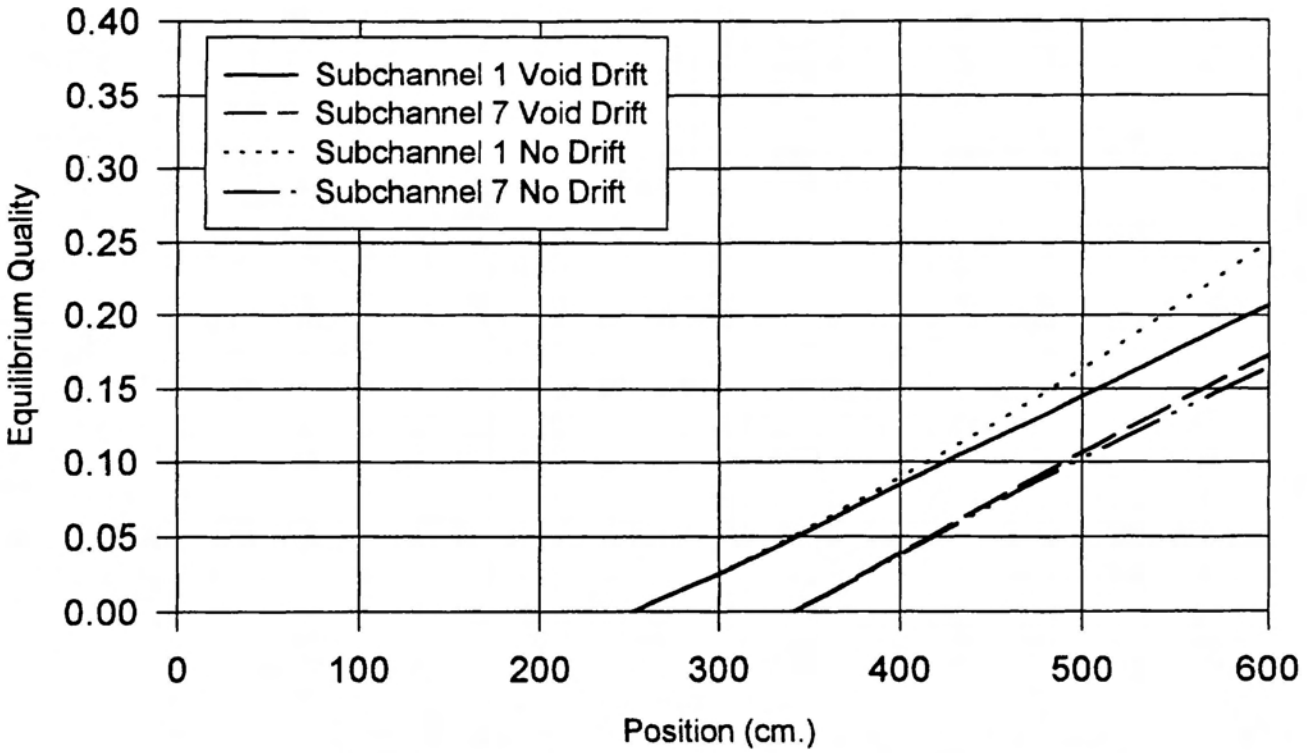

Figure 6. Influence of Void Drift on Subchannel Quality
P=10.0 MPa, G=2.0 Mg/m^2/s, T_{in}=260 °C
Vertical Flow

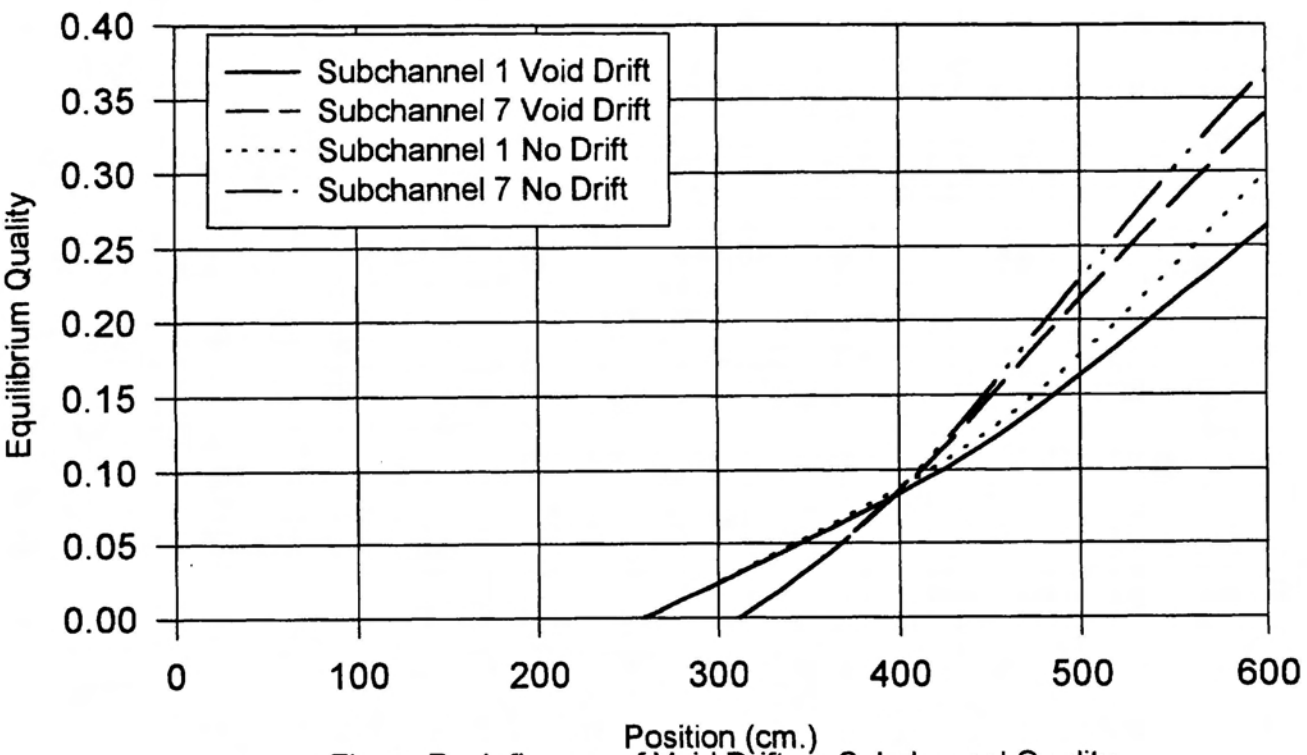

Figure 7. Influence of Void Drift on Subchannel Quality
P=10.0 MPa, G=2.0 Mg/m^{2}s, T_{in}=260 °C
Horizontal Flow

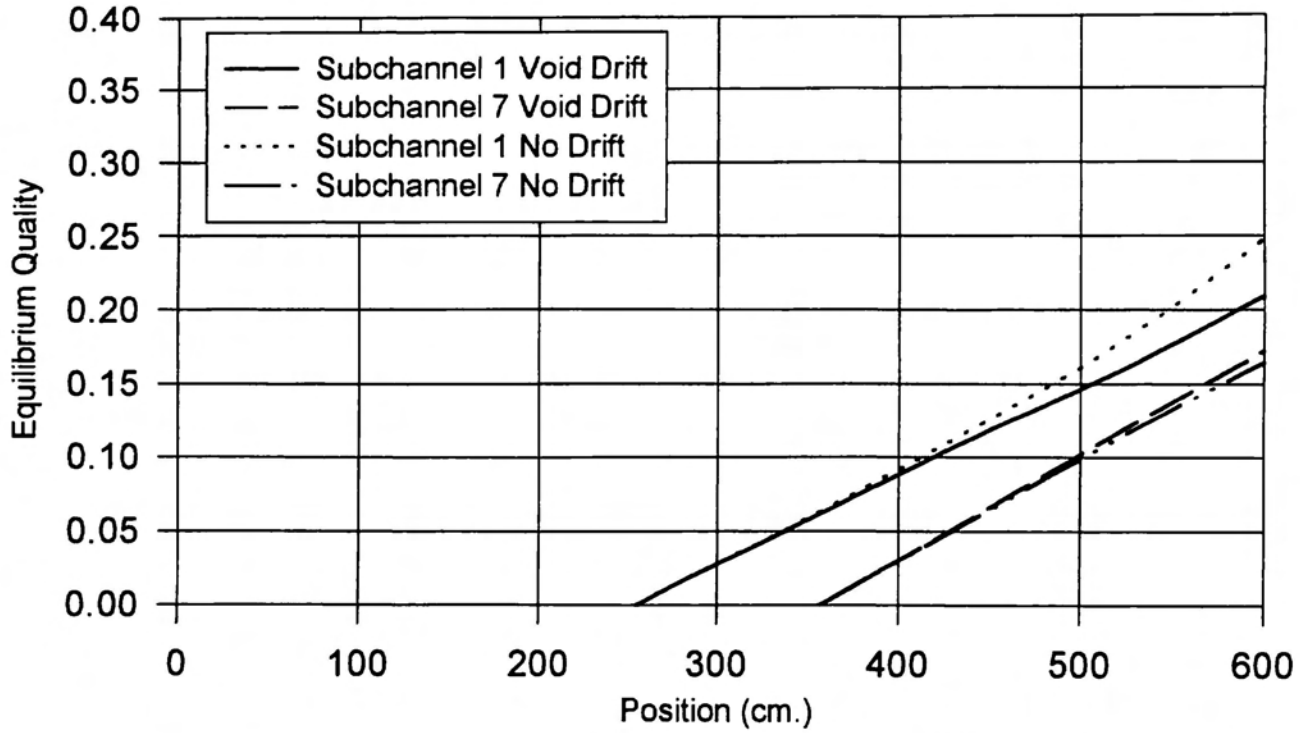

Figure 8. Influence of Void Drift on Subchannel Quality
P=10.0 MPa, G=6.0 Mg/m^2/s, T_{in}=260 °C
Vertical Flow

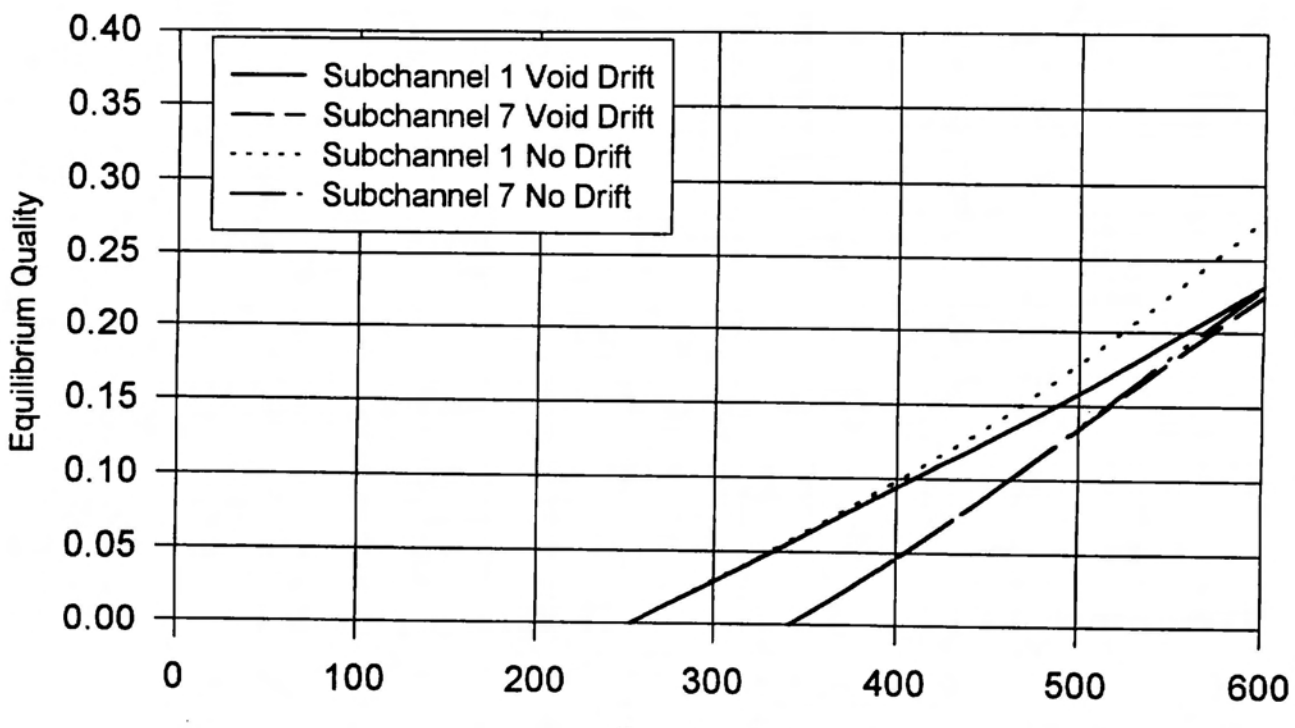

Figure 9. Influence of Void Drift on Subchannel Quality
P=10.0 MPa, G=6.0 Mg/m^{2}s, T_{in}=260 °C
Horizontal Flow

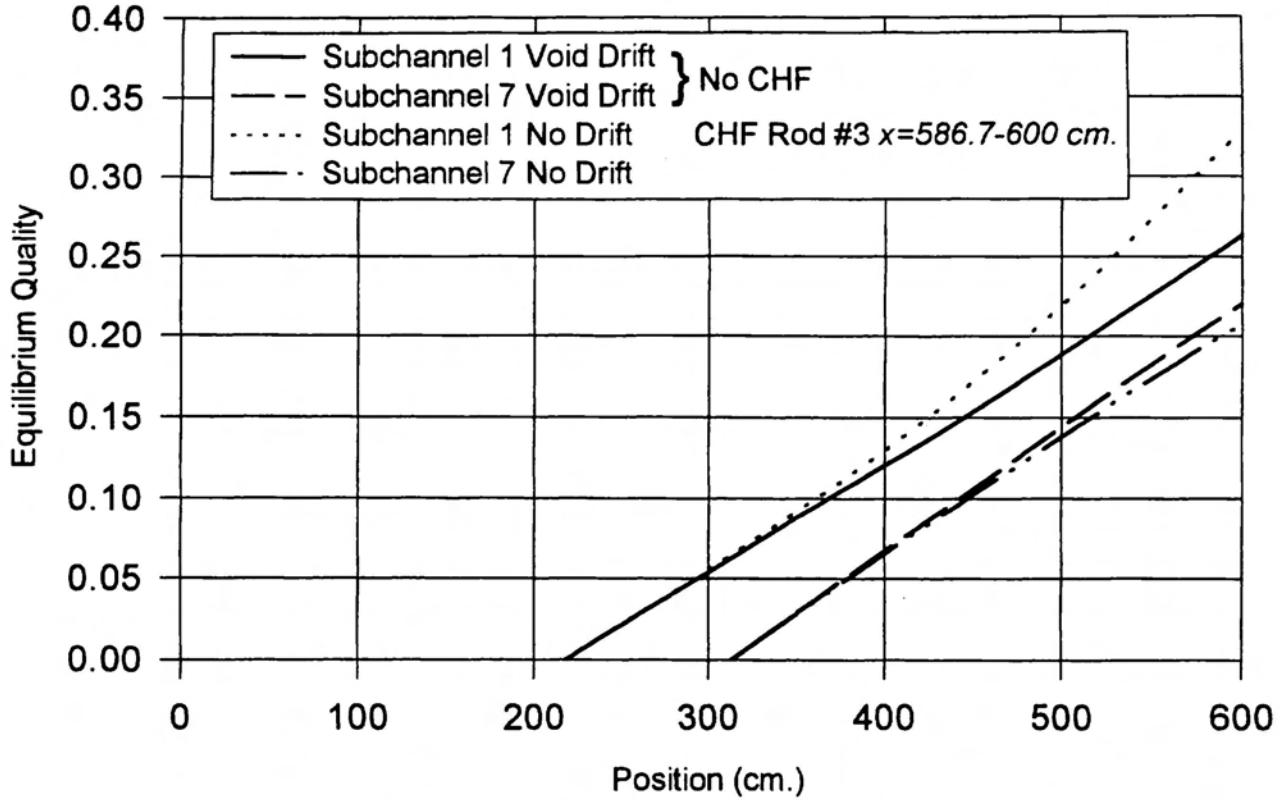

Figure 10. Influence of Void Drift on Subchannel Quality
P= 10 MPa, G=4.0 Mg/m^2/s, T_{in} = 260 °C
Vertical Flow (CHF)

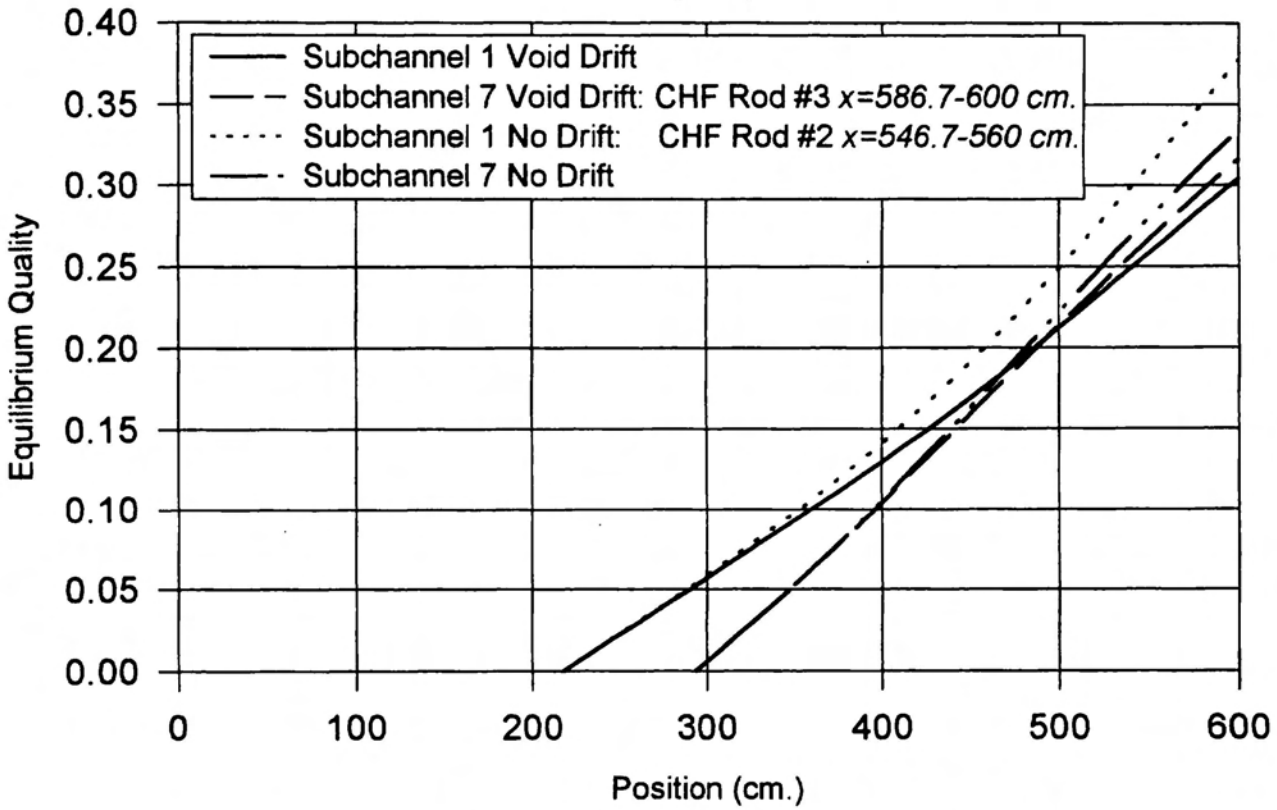

Figure 11. Influence of Void Drift on Subchannel Quality
P= 10 MPa, G=4.0 Mg/m^2/s, T_{in} = 260 °C
Horizontal Flow (CHF)

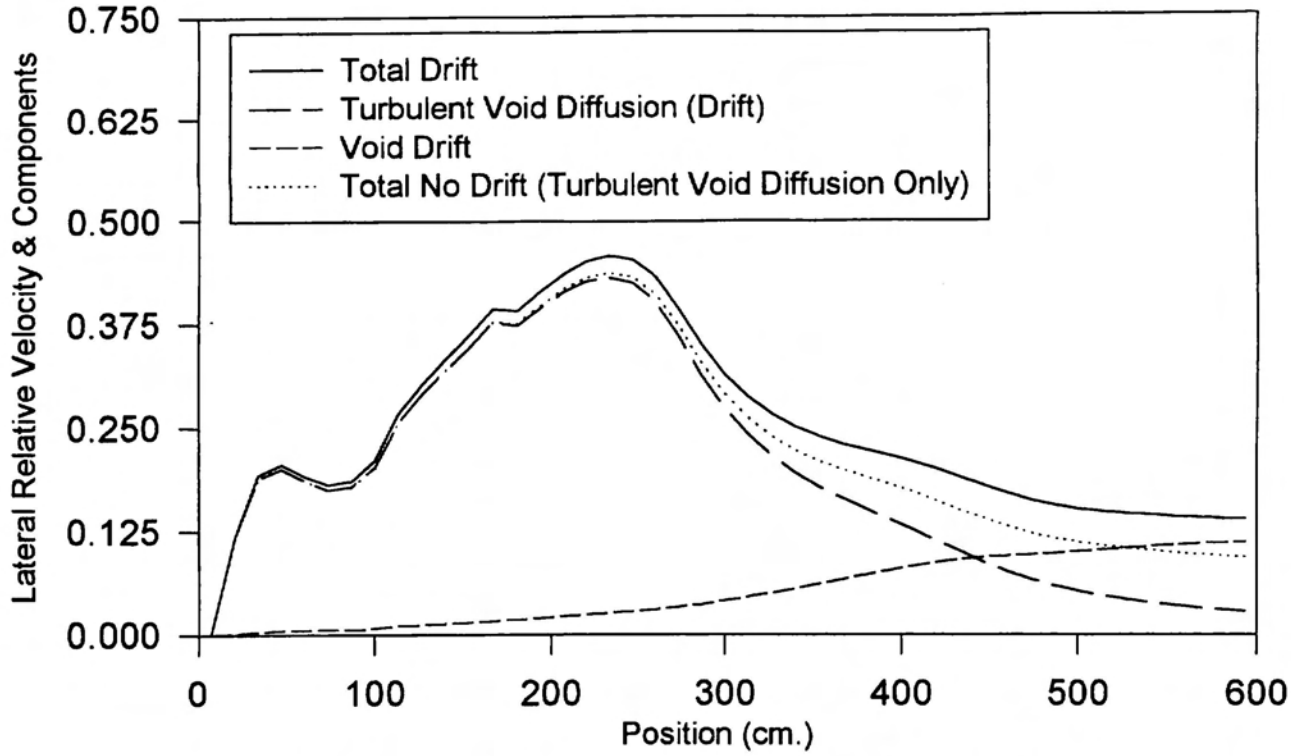

Figure 12. Influence of Void Drift on Lateral Relative Velocity
P=10 MPa, G=4.0 Mg/m^{2}s, T_{in}=260°C
Vertical Flow

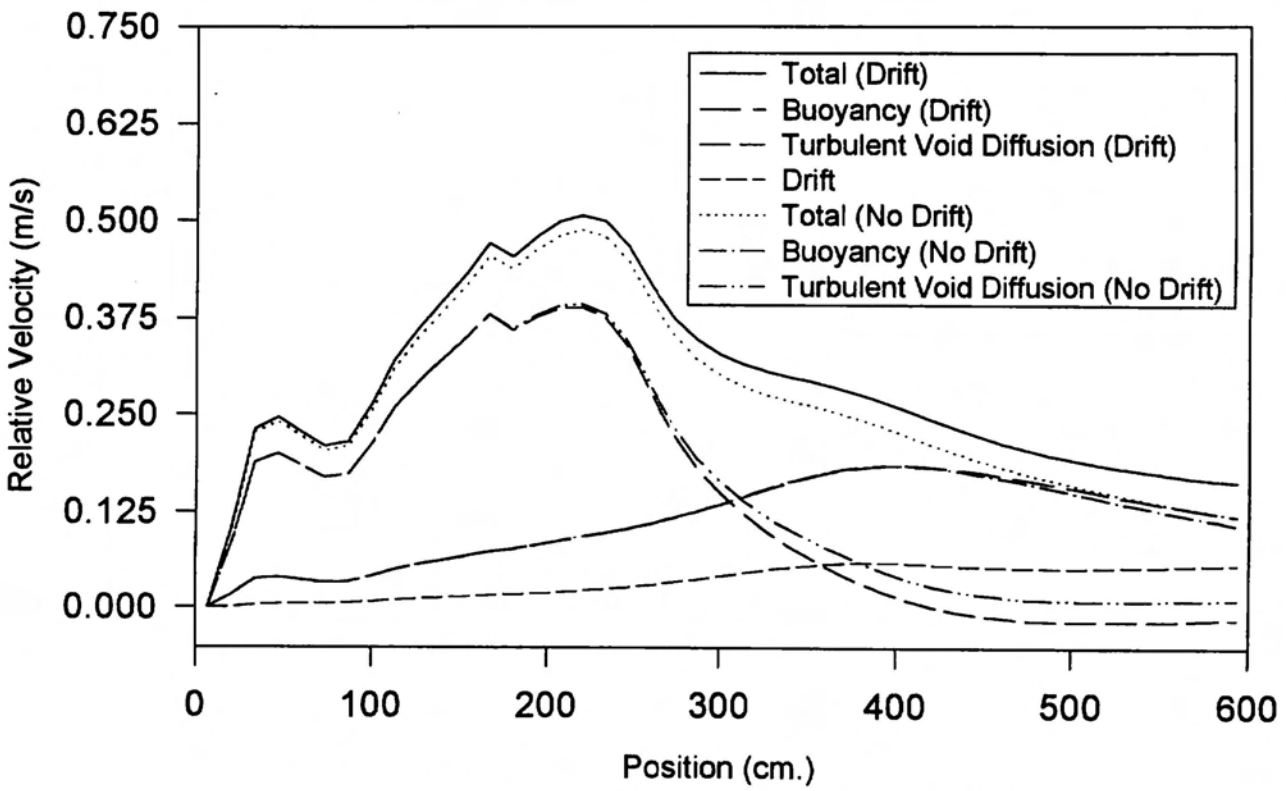

Figure 13. Lateral Relative Velocity and Components
Subchannel 1-7, P=10 Mpa, G=4.0 Mg/m^{2}s, T_{in}=260 °C
Horizontal Flow (CHF)